Developing a Lower Limb Lymphedema Animal Model with Combined Lymphadenectomy and Low-dose Radiation

Chin-Yu Yang, MSc*
Dung H. Nguyen, MD†
Chih-Wei Wu, MD*
Yu-Hua Dean Fang, PhD‡
Ko-Ting Chao, MSc‡
Ketan M. Patel, MD*
Ming-Huei Cheng, MD, MBA*

Background: This study was aimed to establish a consistent lower limb lymphedema animal model for further investigation of the mechanism and treatment of lymphedema.

Methods: Lymphedema in the lower extremity was created by removing unilateral inguinal lymph nodes followed by 20, 30, and 40 Gy (groups IA, IB, and IC, respectively) radiation or by removing both inguinal lymph nodes and popliteal lymph nodes followed by 20 Gy (group II) radiation in Sprague-Dawley rats (350–400 g). Tc^{99} lymphoscintigraphy was used to monitor lymphatic flow patterns. Volume differentiation was assessed by microcomputed tomography and defined as the percentage change of the lesioned limb compared to the healthy limb.

Results: At 4 weeks postoperatively, 0% in group IA ($n = 3$), 37.5% in group IB ($n = 16$), and 50% in group IC ($n = 26$) developed lymphedema in the lower limb with total mortality and morbidity rate of 0%, 56.3%, and 50%, respectively. As a result of the high morbidity and mortality rates, 20 Gy was selected, and the success rate for development of lymphedema in the lower limb in group II was 81.5% ($n = 27$). The mean volume differentiation of the lymphedematous limb compared to the health limb was 7.76% ± 1.94% in group II, which was statistically significant compared to group I ($P < 0.01$).

Conclusions: Removal of both inguinal and popliteal lymph nodes followed by radiation of 20 Gy can successfully develop lymphedema in the lower limb with minimal morbidity in 4 months. *(Plast Reconstr Surg Glob Open 2014;2:e121; doi: 10.1097/GOX.0000000000000064; Published online 14 March 2014.)*

Lymphedema is a debilitating condition that is characterized by the abnormal collection of fluid and proteins within the interstitium. Dysfunctional lymphatic vessels cause lymphatic fluid stasis, decreased macrophage function, and chronic inflammation and fibrosis.[1] It is often a surgical complication following oncologic resection and lymph node dissection. Approximately 16–39% of breast cancer and 20–49% of genital cancer patients suffer from upper extremity lymphedema and

lower extremity lymphedema, respectively.[2,3] The management of lymphedema is complex and includes decongestive physiotherapy and various surgical options. However, no option has been shown to be completely effective and most may provide only temporary relief of symptoms.

Evolving surgical techniques in the management of extremity lymphedema have shown promise with lymphovenous bypass and vascularized lymph node (VLN) flap transfer procedures.[4,5] In our clinical series,[3,6,7] VLN flap transfer from groin area has been shown to effectively improve the lymphatic drainage from lymphedematous limbs in patients with postmastectomy upper extremity lymphedema.

To further investigate effective management strategies for the treatment of lymphedema, a stable and reproducible animal model is needed. Currently, lymphedema models have been previously established in various animal models. In canine and sheep models, variable removal of popliteal lymph nodes and connected lymphatic vessels were performed to replicate lymphedema in the hind limb.[8,9] In Lähteenvuo's porcine model, lymphatic vessel stripping was performed only to identify lymphatic vessels connected to lymph nodes.[10] In a forelimb model, Mendez et al[11] dissected axillary lymph nodes to develop lymphedema. In a hind limb model proposed by Kanter et al,[12] radiation therapy of 45 Gy was coupled with the removal of lymph nodes to replicate lymphedema. Among these models, the hind limb location of the rat model is economically and technically reproducible allowing for further investigation of the surgical treatment of chronic lymphedema. But, previous studies using this model have not shown reproducible lymphedema and have used imprecise limb circumference measurement techniques.[12]

The purpose of this study was to establish a consistent hind limb lymphedema model by combining lower limb lymphadenectomy and assessing effects with differing doses of radiation therapy. In addition, microcomputed tomography (micro-CT) imaging was used to precisely evaluate volumetric changes

of lymphedematous and contralateral healthy limbs. Lymphoscintigraphy was then used to assess lymphatic drainage patterns.

MATERIALS AND METHODS

Lymphedema Rat Model

Male Sprague-Dawley rats (350–400 g) were purchased from BioLASCO Taiwan (Taipei, Taiwan), and all animal procedures were performed and complied with Chang Gung Memorial Hospital Animal Research Guidelines. Rats were divided into different groups: group I, included rats that had removal of inguinal lymph nodes only (Fig. 1). Radiation tolerance was established with variable doses to determine morbidity and mortality. Group II included removal of both inguinal and popliteal lymph nodes (Fig. 2), with the addition of the established dose of radiation therapy.

Isoflurane (2–2.5%) was used as anesthetic for all procedures. Following subcutaneous injection of 0.1 mL of 10% Evans blue (Sigma-Aldrich, Saint Louis, Mich.) into the dorsum of paw, an obliquely oriented incision was made in the midportion of the groin. Lymphatic vessels, inguinal lymph nodes, and popliteal nodes were identified using Evans blue dye staining. The groin fat pad (4×2 cm) was completely resected to remove the inguinal lymph nodes. Along the dyed lymph vessel, popliteal lymph node could be found and resected (Figs. 2B, C). One week after lymphadenectomy, rats were treated with different radiation doses, 20, 30, and 40 Gy radiation as a single dose (Varian 2100 EX Linear Accelerator; Medical Imaging Resources, Ann Arbor, Mich.), with the effective field of 3×4 cm and a depth of 1.5 cm. Lymphedema formation was quantitatively evaluated by micro-CT imaging per month. The rats were followed up for 4 months.

CT Imaging Study

Rat hind limb volume was measured with micro-CT imaging preoperatively and every month following radiation treatment for 4 months. After general anesthesia with isoflurane was induced, animals were imaged with the NanoSPECT/CT (Bioscan, Washington, D.C.) in a supine position. The 8-cm transaxial field of view (FOV) was capable of imaging both extremities and lower abdomen. A 15-minute scan was performed for all CT images (65 kVp, exposure time of 1000 ms, and 123 μA). Approximate radiation exposure was 22 mGy, which has been shown to not cause any known biological damage to the animal.[13] Micro-CT scan images were reconstructed with filtered back-project
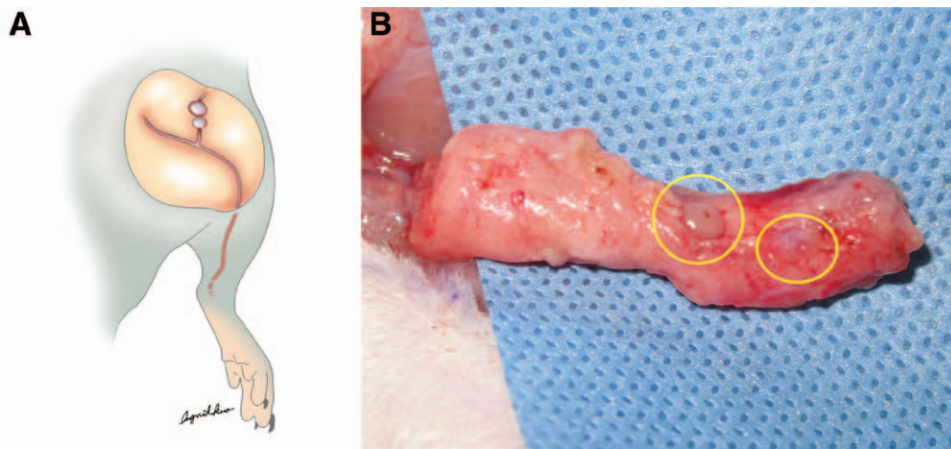
Fig. 1. A, The schematic drawing of inguinal lymph nodes of left limb for removal. B, The left inguinal lymph nodes were identified (yellow circles).
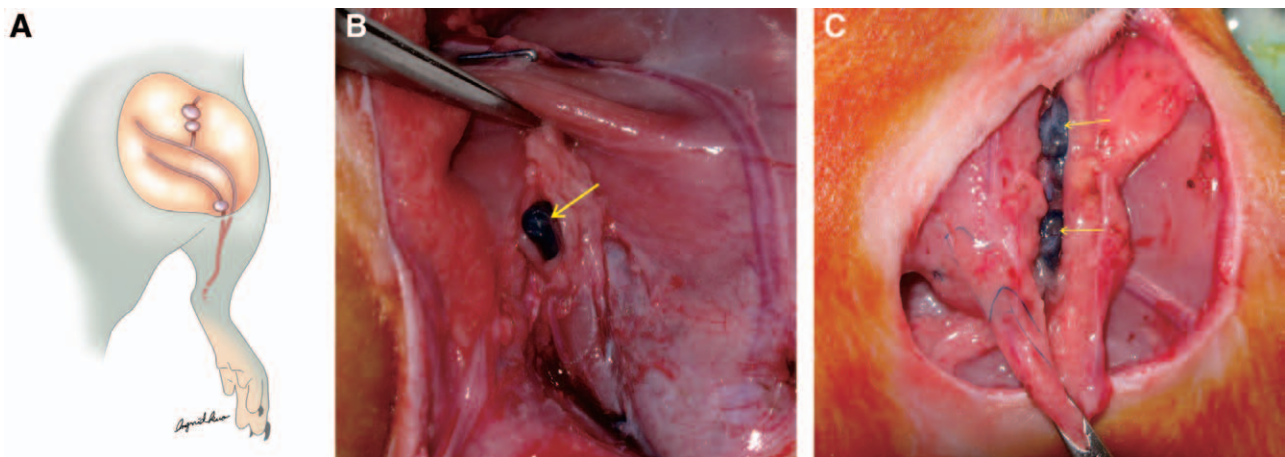

Fig. 2. A, Ten percent (0.1 mL) of Evans blue was injected into the subcutaneous of the paw to indentify popliteal and inguinal lymph nodes and lymph vessels. B, The blue pigmentation was identified in popliteal lymph nodes, which were resected afterward. C, The blue dye was found in the lymphatic duct followed by the inguinal lymph nodes, which were resected completely.

into a 3D-image volume with pixel size of 0.2 mm in both the transverse and axial directions. All images were saved in Digital Imaging and Communications in Medicine (DICOM) format and later analyzed with appropriate software (PMOD Technologies, Zurich, Switzerland). The imaging analysis was performed by an experienced staff with the following steps. First, after images were loaded into PMOD, images of one limb were rotated and realigned so that the cross-sectional images were perpendicular to the tibia. Second, a spherical mask was placed upon the thigh to delineate the thigh from the abdomen. Once that is done, an automatic segmentation was performed with PMOD segmentation capability (Fig. 3). Volume of the segmented limb was computed automatically and exported from PMOD. Following this, the same procedure was repeated for the other limb. As a result, the volume of each limb was calculated and later used in the

statistical analysis to evaluate the lymphedematous extremity. Then, the volume differentiation could be calculated, which was defined as the volume of the lesioned limb minus the volume of the healthy limb and then divided by the volume of the healthy limb multiplied by 100.

Lymphoscintigraphy

Tc[99] nanocolloid was performed to evaluate the function of the lymphatic system in the lower extremities in 2 rats in each group. The same NanoSPECT/CT camera was used for the data acquisition by using the SPECT camera to image animals in a 2D planar scintigraphy mode. For each animal, 0.5 mCi of Tc[99] nanocolloid was injected subcutaneously in the paw of each side. The tracer volume was 0.1 mL. The image acquisition was performed with 3 separate scans. Immediately after injection, a dynamic planar acquisition was started with 10 seconds per frame for 30
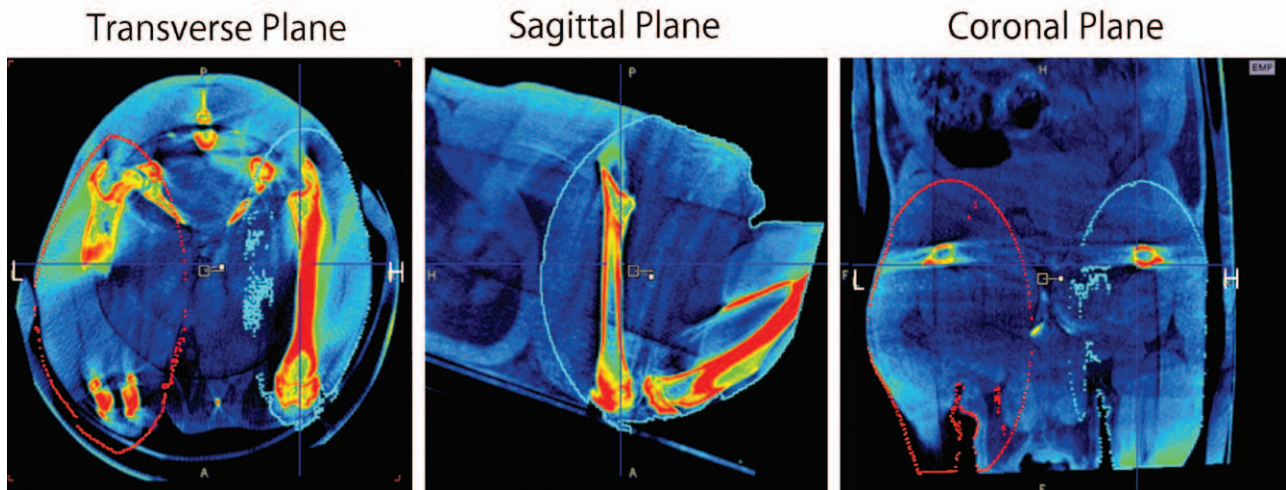
Fig. 3. The micro-CT images of rats were taken 1 month post surgery and radiation. The micro-CT images were reconstructed for volume calculation from the ankle joint to the hip joint, with transverse, sagittal, and coronal sections. The lesioned (L) and healthy limbs (H) were marked by the red and blue circles, respectively.

minutes. The 25-cm field of view of the SPECT acquisition covers the lung, the heart, the abdomen, the lower limbs, and the injection sites. After this scan, the animal was taken off the scanner and anesthetized. At the fifth hour post injection, the animal was rescanned with sixty 10-second frames for 10 minutes and then taken off the scanner. Image acquisition was repeated again for the same animal at 24-hour post injection with 20-minute acquisition of 120 10-second frames. The images were again analyzed with PMOD.

Statistical Analyses

The data were analyzed and compared using the Kruskal-Wallis test. Results were expressed as mean ± SD. A P-value of less than 0.05 was used as the criterion for statistical significance.

RESULTS

Lymphedema Rat Model

A total of 71 rats were used, and the mortality and morbidity rate was 38%. The overall success rate of development of lower limb lymphedema was 57.7%. Success rate in the development of lymphedema was highest in group IC (50%) compared to group IB (37.5%) and group IA (0%) (Table 1). As a result of higher total morbidity and mortality rates in groups IB (56.3%) and IC (50%), we removed both inguinal lymph nodes and popliteal lymph nodes that were identified by injection of Evans blue (Fig. 2) and treated with 20 Gy radiation (group II) with minimal morbidity for evaluating the effect of developing hind limb lymphedema (Fig. 3). The results showed that the success rate of development of hind limb lymphedema in group II was higher (22/27, 81.5%) than group I, and the volume differentiation in group II was 7.76% ± 1.94% ($P < 0.01$). In addition, we followed up the survived rats for 4 months, with the volume differentiation maintaining around 5%.
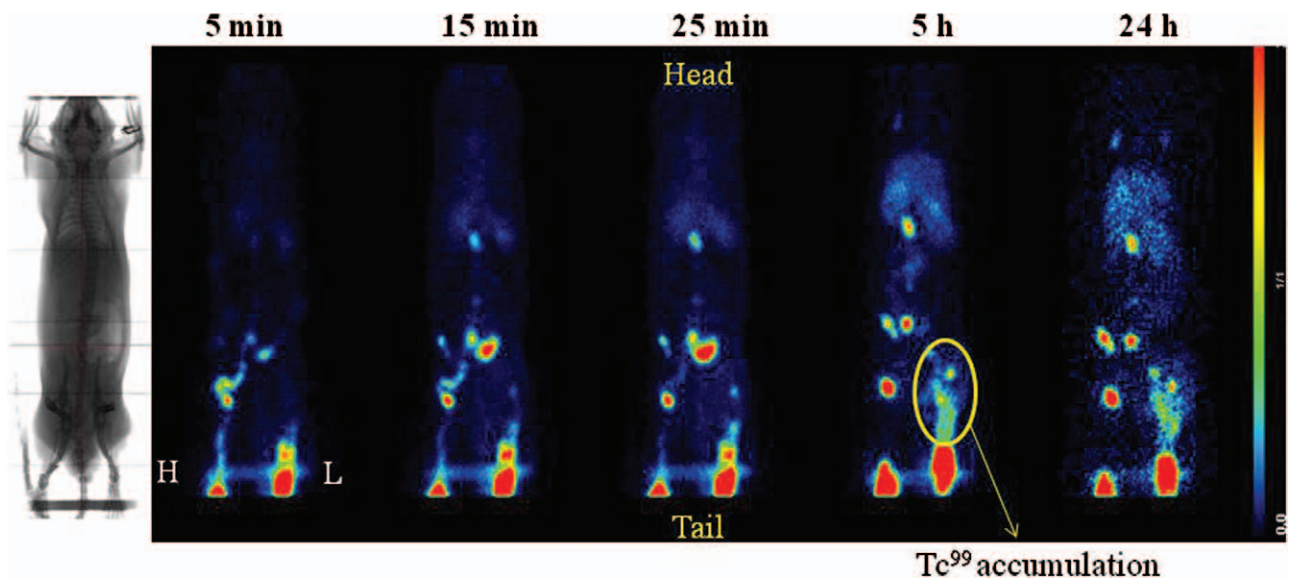
Lymphoscintigraphy Image

Lymphoscintigraphy was used to verify the lymphatic drainage every month postoperatively for 3 months. The image was detected after 5 minutes, 15 minutes, 25 minutes, 5 hours, and 24 hours following Tc[99] nanocolloid injection. The Tc[99] signal was seen in green and red colors. The results showed that the position of lymph nodes could be seen in

Table 1. The Success Rate of Development of Hind Limb Lymphedema in Different Treatment Modalities

Group	No. Cases	Lymph Nodes Removed	Radiation Dose (Gy)	Cases of Development of Lymphedema (%)	Complications		
					Morbidity (%)	Mortality (%)	Total (%)
IA	3	Inguinal LNs	20	0 (0)	0 (0)	0 (0)	0 (0)
IB	15		30	6 (37.5)	8 (50.0)	1 (6.5)	9 (56.3)
IC	26		40	13 (50.0)	6 (23.1)	7 (26.9)	13 (50)
II	27	Inguinal and popliteal LNs	20	22 (81.5)*	0 (0)	0 (0)	0 (0)

*p (lower case) < 0.01.
LN, lymph nodes.

Fig. 4. Tc99 nanocolloid lymphoscintigraphy results after 3 months of development of lymphedema. The images were taken at 5 min, 15 min, 25 min, 5 h, and 24 h. Yellow circle indicated the accumulation of Tc^{99} nanocolloid. The lesioned limb was marked as L and healthy limb as H.

the healthy limb in 5 minutes. However, after 5 and 24 hours, the Tc^{99} nanocolloid was accumulated in the lesioned limb in the group II (Fig. 4).

DISCUSSION

The importance of developing a reliable and consistent animal model to investigate extremity lymphedema is particularly valuable as clinical treatment modalities continue to improve. As awareness of this disease process continues, translating clinical parameters to an animal model will allow clinicians to investigate and optimize treatment strategies. Previous small animal models have been described and investigated.[12,14–17] But, inconsistencies in results and methodology make these difficult to implement in the experimental setting. In addition, the quantification methods were inconsistent and inaccurate in previous studies. Therefore, we modified the structural techniques from previous studies.[12,18]

First, to determine a consistent radiation dose, varying doses of radiation therapy were used (20, 30, and 40 Gy) to treat the inguinal lymph nodes removed in rats. Although 40 Gy would have the highest success rate for developing lower limb lymphedema, this dose proved to be too toxic causing a high rate of morbidity and mortality. In a similar model described by Kanter et al,[12] a 5- to 10-mm skin gap was left during wound closure. The inflammatory response induced appreciable acute lymphedema in the rat hind limb after 2 days. In our model, no skin gap is left and direct skin closure is performed. In addition, 45 Gy was used with success in the de-

velopment of lymphedema in the previous rat hind limb model.[12] Although successful in their initial study, we found this dose to be toxic with considerable morbidity. The lower radiation dose (20 Gy) did not create significant toxicity but was unable to initiate lower limb lymphedema with isolated inguinal lymph node removal. Therefore, both inguinal and popliteal lymphadenectomy were performed with the addition of a lower radiation dose. This sequence proved to be successful in creating a lymphedematous extremity.

In addition to the modified technique for improving induction of lymphedema, volume differentiation between limbs determined by micro-CT images proved to be successful and precise in evaluating volumetric parameters in rats. In a previously reported lymphedema model, volume estimations were made by limb circumference measurements and water displacement volumetry,[12,15,17] but the studies showed high variability between control and the lymphedema areas. In another study, T2-weighted magnetic resonance imaging was also used for measuring the volume of the fluid accumulation in the subcutaneous tissue, but this methodology has significant associated costs.[19] In the presented study, micro-CT was able to accurately and reliably determine volume differentiation between lesioned and healthy limbs with the benefit of decreased costs compared to magnetic resonance imaging. In addition, for specific evaluation of lymphatic flow, lymphoscintigraphy by injected Tc^{99} nanocolloid was effective at determining the success of lymphadenectomy and progression to lymphedema. These combined imaging techniques

will make it possible to determine the physiologic basis of treatment strategies such as VLN transfer.

CONCLUSIONS

In this study, we successfully used low radiation doses combined with the removal of inguinal and popliteal lymph nodes to develop lymphedema in the lower limb up to 4 months with minimal donor-site morbidity. The utilization of micro-CT to assess volumetric changes of the lymphedema in the rat model is reproducible and accurate.

Ming-Huei Cheng, MD, MBA
Division of Reconstructive Microsurgery
Department of Plastic and Reconstructive Surgery
Chang Gung Memorial Hospital
Chang Gung University
Collage of Medicine
Taoyuan
Taiwan
E-mail: minghuei@cgmh.org.tw

REFERENCES

1. Warren AG, Brorson H, Borud LJ, et al. Lymphedema: a comprehensive review. *Ann Plast Surg.* 2007;59:464–472.
2. Hadamitzky C, Pabst R. Acquired lymphedema: an urgent need for adequate animal models. *Cancer Res.* 2008;68:343–345.
3. Lin CH, Ali R, Chen SC, et al. Vascularized groin lymph node transfer using the wrist as a recipient site for management of postmastectomy upper extremity lymphedema. *Plast Reconstr Surg.* 2009;123:1265–1275.
4. Yamamoto T, Koshima I, Yoshimatsu H, et al. Simultaneous multi-site lymphaticovenular anastomoses for primary lower extremity and genital lymphoedema complicated with severe lymphorrhea. *J Plast Reconstr Aesthet Surg.* 2011;64:812–815.
5. Chang DW. Lymphaticovenular bypass for lymphedema management in breast cancer patients: a prospective study. *Plast Reconstr Surg.* 2010;126:752–758.
6. Cheng MH, Chen SC, Henry SL, et al. Vascularized groin lymph node flap transfer for postmastectomy upper limb lymphedema: flap anatomy, recipient sites, and outcomes. *Plast Reconstr Surg.* 2013;131:1286–1298.
7. Cheng MH, Huang JJ, Nguyen DH, et al. A novel approach to the treatment of lower extremity lymphedema by transferring a vascularized submental lymph node flap to the ankle. *Gynecol Oncol.* 2012;126:93–98.
8. Chen HC, O'Brien BM, Rogers IW, et al. Lymph node transfer for the treatment of obstructive lymphoedema in the canine model. *Br J Plast Surg.* 1990;43:578–586.
9. Tobbia D, Semple J, Baker A, et al. Lymphedema development and lymphatic function following lymph node excision in sheep. *J Vasc Res.* 2009;46:426–434.
10. Lähteenvuo M, Honkonen K, Tervala T, et al. Growth factor therapy and autologous lymph node transfer in lymphedema. *Circulation* 2011;123:613–620.
11. Mendez U, Stroup EM, Lynch LL, et al. A chronic and latent lymphatic insufficiency follows recovery from acute lymphedema in the rat foreleg. *Am J Physiol Heart Circ Physiol.* 2012;303:H1107–H1113.
12. Kanter MA, Slavin SA, Kaplan W. An experimental model for chronic lymphedema. *Plast Reconstr Surg.* 1990;85:573–580.
13. Badea CT, Drangova M, Holdsworth DW, et al. In vivo small-animal imaging using micro-CT and digital subtraction angiography. *Phys Med Biol.* 2008;53:R319–R350.
14. Mendez U, Brown EM, Ongstad EL, et al. Functional recovery of fluid drainage precedes lymphangiogenesis in acute murine foreleg lymphedema. *Am J Physiol Heart Circ Physiol.* 2012;302:H2250–H2256.
15. Serizawa F, Ito K, Matsubara M, et al. Extracorporeal shock wave therapy induces therapeutic lymphangiogenesis in a rat model of secondary lymphoedema. *Eur J Vasc Endovasc Surg.* 2011;42:254–260.
16. Pan D, Han J, Wilburn P, et al. Validation of a new technique for the quantitation of edema in the experimental setting. *Lymphat Res Biol.* 2006;4:153–158.
17. Liu Y, Fang Y, Dong P, et al. Effect of vascular endothelial growth factor C (VEGF-C) gene transfer in rat model of secondary lymphedema. *Vascul Pharmacol.* 2008;49:44–50.
18. Ogata F, Azuma R, Kikuchi M, et al. Novel lymphography using indocyanine green dye for near-infrared fluorescence labeling. *Ann Plast Surg.* 2007;58:652–655.
19. Sommer T, Meier M, Bruns F, et al. Quantification of lymphedema in a rat model by 3D-active contour segmentation by magnetic resonance imaging. *Lymphat Res Biol.* 2012;10:25–29.